Renewable and Sustainable Energy Reviews 94 (2018) 931–944

Contents lists available at ScienceDirect

Renewable and Sustainable Energy Reviews

journal homepage: www.elsevier.com/locate/rser

Current trends in surface tension and wetting behavior of nanofluids

Patrice Estellé[a,*], David Cabaleiro[b,c], Gawel Żyła[d], Luis Lugo[b], S.M. Sohel Murshed[e,f]

[a] LGCGM, Matériaux et Thermo-Rhéologie, Université Rennes 1, 35704 Rennes Cedex 7, France
[b] Dpto. Física Aplicada, Facultade de Ciencias, Universidade de Vigo, 36310 Vigo, Spain
[c] National Research Council, Institute of Construction Technologies, Corso Satti Uniti 4, 35127 Padova, Italy
[d] Department of Physics and Medical Engineering, Rzeszow University of Technology, Rzeszow, Poland
[e] Centro de Quimica Estrutural, Faculdad de Ciências, Universidad de Lisboa, 1749-016 Lisboa, Portugal
[f] Centre for Innovation, Technology and Policy Research, Instituto Superior Técnico, Universidade de Lisboa, 1049-001 Lisboa, Portugal

ARTICLE INFO

Keywords:
Nanofluids
Surface tension
Wettability
Nanoparticle influence
Effect of temperature
Heat transfer

ABSTRACT

Nanofluids are recent nanomaterials with improved thermophysical properties that could enhance the efficiency and reliability of heat transfer systems. Relevant properties for heat transfer calculation, thin film flows, droplet impingements or microfluidic are surface tension and wettability. However, to date, the understanding of those properties in nanofluids field is at the beginning compared to transport properties. At this stage, this review focus on the effect of nanoparticles and base fluid nature, temperature, use of surfactant, nanoparticle concentration, size and shape as well on the surface tension and wettability of nanofluids. After the presentation of heat transfer processes involving the influence of surface tension and wettability, this paper is organized according to the nature of the nanoparticles dealing with oxide, carbon-based and metallic nanofluids as well as unusual or less considered nature of nanoparticles. The factors affecting the surface tension of nanofluids are relatively well identified, but concentration and surfactant effects present some inconsistent outcomes. In any case, the dispersion of nanoparticles have an effect on the surface tension of base fluid significantly lower than that on transport properties. Based on results available in the literature and existing empirical correlations, a comprehensive assessment, challenges and future works are suggested.

1. Introduction

The surface tension (ST) of thermal fluids is of great importance when analyzing the performance of thermal systems since this physical property influences the surface wettability and bubble growth. Hence, ST is, together with the vaporization latent heat and the density difference between liquid and vapor phases, the most important parameters in order to describe boiling and condensation processes [1].

In a non-dimensional analysis of boiling heat transfer flows, ST appears in the Bond number (Bo), which represents the ratio of the buoyancy forces to the surface tension forces. If the Bo value is high, the working fluid is supposed to boil vigorously [2]. Hence, a reduction in ST is expected to enhance the boiling flow heat transfer performance. ST is also present in most of the correlations proposed in literature for nucleate pool boiling [3], particularly at critical heat flux conditions [4,5]. According to these equations, nucleate boiling heat flux can be enhanced by reducing surface tension [6]. Regarding external forced boiling such as in a fire tube boiler, Lienhard and Eichhorn [7] developed expressions for low and high velocity flows. In both situations, a reduction in ST leads to an increase in Weber number and a diminution of convective heat flux [6]. Recently, Fang et al. [8] and Ciloglu and Bolukbasi [9] reviewed main literature outcomes concerning nanofluid performance under flow boiling the former and nucleate boiling the later. Both works underline the importance of ST to understand flow patterns and bubble dynamics under boiling. Authors such as Vafei et al. [10] pointed out that the addition of nanoparticles can play even a double role. Thus, suspended particles modify bubble dynamics significantly by varying contact angles, departure bubble volume, and frequency, while nanoparticle deposited on the heating surface modify surface wettability and reduce thermal resistance of evaporator and condenser.

Heat pipes are heat-transfer devices currently used in cooling management of electronics and computers. These capillary structures consist of a tube closed at both ends that combines the principles of high thermal conductivity and phase transition to effectively transfer thermal energy between two solid interfaces when subjected to a temperature difference [11]. The capillary effect consequence of the surface tension of the working fluid can lead to a liquid transference from the condenser to evaporator, which in turn can influence the increase in thermal performance of heat pipes. Correlations for predicting

* Corresponding author.
E-mail address: patrice.estelle@univ-rennes1.fr (P. Estellé).

https://doi.org/10.1016/j.rser.2018.07.006
Received 30 November 2017; Accepted 1 July 2018

Nomenclature

Abbreviations

ST	Surface tension
IT	Interfacial tension
W	Wetting behavior or Wettability
CA	Contact Angle
CMC	Critical micelle concentration
CTAB	Cetyltrimethyl ammonium bromide
DIW	Distilled water
DG	Diethylene glycol
DTAB	Dodecyltrimethyl-ammonium bromide
EG	Ethylene glycol
G	Graphene
GO	Graphene oxide
PDMS	Polydimethylsiloxane
PEG	Polyethylene glycol
PTFE	Polytetrafluoroethylene
PVP	Polyvinylpyrrolidone
SDS	Sodium dodecyl sulfate
SDBS	Sodium dodecyl benzene sulfonate
T	Temperature
TEG	Triethylene glycol
ϕ	Nanoparticle loading (in wt%, vol%, g/l or ppm)
γ	Surface tension
np	nanoparticle
bf	base fluid
nf	nanofluid
↑	Increase
↓	Decrease
→	Constant

the heat transfer of heat pipes such as that proposed by Kim and Peterson [12] require the knowledge of surface tension. There, Weber number is used to explain the counter-current interactions between free surface of liquid film and vapor flows inside the operating heat pipe, and provides a convenient measure of the likelihood of liquid entrainment [2].

Two-phase closed thermosiphons (TPCT) are thermodynamically similar to wicked heat pipes with gravity-assisted liquid-vapor flows. The maximum heat flux inside the evaporator of a thermosiphon can be expressed in a dimensionless way through Kutateladze number [13], which is usually correlated as a function of Bond number [2,14]. Like with the rest of heat pipes, the main research areas to enhance the performance of TPCTs are focused on the necessity of a better wick development to minimize entrainment and optimizing the fluid design [2]. In this sense, it is well known that reductions in ST can improve TPCT performance [15]. Liu and Li [16] and Gupta et al. [17] reviewed and summarized previous research on heat pipes using nanofluids as working fluids. The majority of nanofluid studies showed a reduction in thermal resistance of heat pipes and thermosiphons with the addition of nanoparticles to the working fluid. Most authors attributed improvements in thermal performance and operating range to modifications in thermal conductivity but also in surface tension, liquid density and latent heat of vaporization.

In recent years, microfluidics and minifluidics have raised increasing attention in heat transfer field due to current trend towards component miniaturization in a wide range of industrial applications. In particular, flow boiling in microchannels has been proposed as a promising cooling method, due to the possibility of achieving very high heat transfer rates with small variations in the surface temperature [18]. According to the classification proposed by Cheng et al. [19] for two-phase channels, Bond number must be below 0.05 for the flow system to be considered as microchannel. These low Bo values indicate

Table 1
Thermal configurations and applications involving surface tension influence.

Type of heat and mass transfer application	Main heat and mass transfer governing equations depending on surface tension	Parameter involving the surface tension	Influence of surface tension
Boiling heat transfer	$Nu = \frac{h \cdot L}{k} = f\left[\frac{\rho \cdot g \cdot (\rho_l - \rho_v) \cdot L^3}{\mu^2}; Pr = \frac{\mu \cdot c_p}{k}; Ja = \frac{\Delta T \cdot c_p}{h_{fg}}; Bo = \frac{g \cdot (\rho_l - \rho_v) \cdot L^2}{\gamma}\right]$ Where Nusselt (Nu), Prandl (Pr), Jacob (Ja) and Bond (Bo) numbers depend on the characteristic length (L), thermal conductivity (k), density (ρ), viscosity (μ), isobaric heat capacity (c_p), excess temperature (ΔT), latent heat of vaporization (h_{fg}), surface tension (γ) and acceleration due to gravity (g). Subscripts stand for liquid (l) and vapor (v).	Heat transfer coefficient (h) and Bond number (Bo) [1]	Bo ↑ and h ↑ if ST ↓
Nucleate pool boiling, Critical heat flux	$q^{"} = \mu_l \cdot h_{fg} \cdot \left(\frac{g \cdot (\rho_l - \rho_v)}{\gamma}\right)^{1/2} \cdot \left(\frac{c_{p,l} \cdot \Delta T}{C_{s,f} \cdot h_{fg} \cdot Pr_l^n}\right)^3$ Where $C_{s,f}$ coefficient and n exponent depend on the solid–liquid combination. $q^{"}_{max} = C \cdot h_{fg} \cdot \rho_v \cdot \left(\frac{\gamma \cdot g \cdot (\rho_l - \rho_v)}{\rho_v^2}\right)^{1/4}$ Where C is a constant depending on heated surface geometry.	Critical heat flux for nucleate boiling (q") [4,5]	q" ↑ if ST ↓
External flow convection	Low velocity: $\frac{q^{"}_{max}}{\rho_v \cdot h_{fg} \cdot V} = \frac{1}{\pi} \cdot \left(1 + \left(\frac{4}{We_D}\right)^{1/3}\right)$ High velocity: $\frac{q^{"}_{max}}{\rho_v \cdot h_{fg} \cdot V} = \frac{(\rho_l / \rho_v)^{3/4}}{169 \cdot \pi} + \frac{(\rho_l / \rho_v)^{1/2}}{19.2 \cdot \pi \cdot We^{1/3}}$ Where $We = (\rho_v \cdot V^2 \cdot D)/\gamma$ is the Weber number, V is the liquid velocity and D is the diameter.	Critical heat flux for external convection boiling (q") and Weber number (We) [7]	We ↑ and q" ↓ if ST ↓
Flow boiling in Microchannels	$K_2 = \left(\frac{q'}{h_{fg}}\right)^2 \cdot \frac{D}{\rho_v \cdot \gamma}; Ca = \frac{\mu \cdot V}{\gamma}$	Kandlikar (K_2) and capillary number (Ca) [23]	Ca ↑ if ST ↓
Heat pipes	$We_{critical} = \frac{\rho_v \cdot v^2 \cdot z}{2 \cdot \pi \cdot \sigma} = 10^{-1.163} \cdot N_{vi}^{0.744} \cdot \left(\frac{\lambda_c}{d_1}\right)^{-0.509} \cdot \left(\frac{D_h}{d_2}\right)^{0.276}$ Where z is a dimension characterising the vapor liquid surface, v is the vapor velocity, N_{vi} is the dimensionless viscosity number, λ_c is the critical wavelength, d_1 is the mesh wire spacing, d_2 is the wire thickness and D_h is the equivalent diameter of the vapor space.	Weber number (We) [12]	We ↑ if ST ↓
Thermosiphons	$Ku = \frac{q_{co}}{(\Delta h_{lv} \cdot \rho_v^{0.5} \cdot (\sigma \cdot g \cdot (\rho_l - \rho_v)^{0.25}))}$	Maximum heat flux (q_{co}) and Kutateladze number (Ku) [13]	Ku ↑, q_{co} ↓ if ST ↓

that gravity effects can be generally ignored in microfluidics [20]. Despite Reynolds (Re) number being the most important dimensionless number in fluid dynamics, Re is not expected to play an important role in microfluidics since inertial forces are considerably lower than viscous forces in this kind of systems. Similarly, Weber number is not practical either to describe flow behavior in microchannels since We < 1 when the flow geometry is downscale in the micron range. The relative strength between viscous and surface tension forces can be expressed through the capillary number, Ca [21]. Thus, low Ca values indicate a predominance of interfacial tension, while the contrary happens for high Ca numbers. Non-mechanical pumping methods such as thermo-capillary and electrocapillary are examples of tension-driven flows in microchannels [22]. Another dimensionless number, which represents the ratio of evaporation momentum to surface tensions forces at the liquid-vapor interface was developed by Kandlikar [23] to model interface motion such as in critical heat flux at the microscale.

Finally, fluids surface tension is also important in analyzing fluids and thin film flows, droplet impingements as well as spray cooling technologies [24]. Based on our analysis reported above, governing equations of heat and mass transfer processes involving surface tension are gathered in Table 1, in which general information about how ST influences heat transfer performance is also provided.

Owing the importance of surface tension in the field of nanofluids, emerging as promising advanced heat transfer fluids, investigation of ST property of these materials is at the early stage compared to transport properties such as thermal conductivity or viscosity [25,26]. At this stage, the main purpose of this paper is to present an overview of research development on surface tension (ST) of nanofluids. In addition, as boiling phenomena of nanofluids can also induce the modification of surface properties, main results about wetting behavior or wettability (W) of nanofluids are also included in this study.

The techniques used for the measurement of ST and W of nanofluids are similar to the ones developed and exploited for common liquids. Hence, the reader can refer to [27] for the description of techniques used for ST evaluation, their limitations and theoretical analysis for the evaluation of these properties. As a reminder, these techniques are shown in Fig. 1 [28]. With regards to W, this property is generally addressed from contact angle measurement largely operated in the literature. It should be noted that the techniques used are also generally described, at least partially, in the literature articles reviewed in this study.

Consequently, this review will focus specifically on the effect of nanoparticle nature, size, shape, concentration, and the influence of base fluid, surfactant content, and temperature on ST and W properties of nanofluids. In addition, some correlations developed or used for ST of nanofluids will be presented. Finally, challenges and future works dedicated to ST and wettability of nanofluids are also suggested.

2. Oxide nanofluids

Various types of oxide nanofluids are used by the researchers for studying their ST and W. In addition to the following description of ST and W studies of oxide nanofluids, details are also provided in Tables 2–5 considering respectively Al_2O_3, TiO_2, SiO_2, and CuO, ZnO, MgO and other oxide nanofluids.

2.1. Al_2O_3 nanofluids

As for thermal and rheological characteristics, Al_2O_3 nanofluids are the most studied nanofluids with regards to their ST properties. First study considering this property was performed in 2003 by Das et al. [29]. It was motivated by the possible ST influence on pool boiling process. Commercial nanoparticles with volume weighted average size of 38 nm were dispersed in water avoiding the use of surfactant in the range 0–4% in volume fraction. ST of Al_2O_3 nanofluids, which was measured from conventional ring method at ambient temperature, was shown to be quite constant with nanoparticle concentration and very close to ST of water.

With the same motivation, influence of nanofluids on surface wettability improvement during pool boiling was investigated by Coursey and Kim [30]. Water and ethanol based nanofluids were studied by the authors, nanofluids being obtained by the dilution with base fluid of commercial solution with unknown quantity of surfactant. Diameter of commercial Al_2O_3 nanoparticles was 45 nm. Range of nanoparticle content was 0.001–10.02 g/l and 0.026–1.02 g/l for ethanol and water, respectively. Contact angle (CA) of pure fluids and nanofluids was measured before and after boiling phenomena considering also the degree of surface oxidation. They reported that poorly wetting

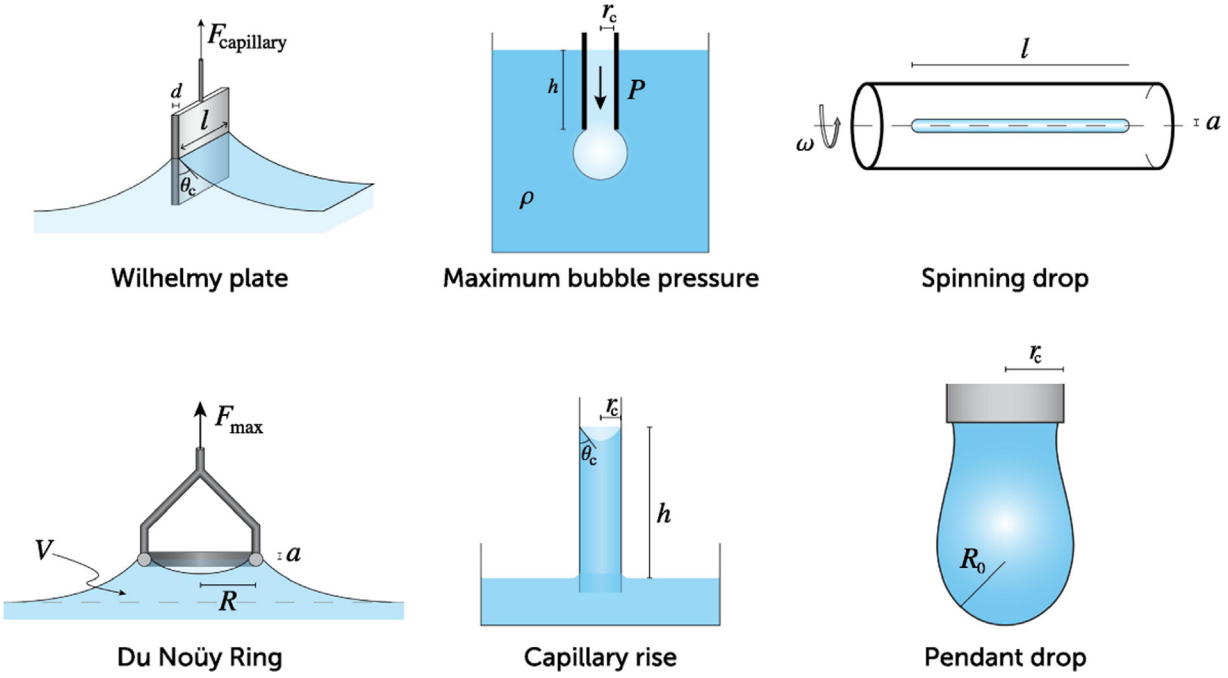

Fig. 1. Main techniques generally used for ST measurement of liquids and nanofluids, extracted from [27].

Table 2
Main informations related to ST and W behavior of Al_2O_3 nanofluids.

Reference	Nanoparticles		Base fluid	Surfactant	Dispersion method	Measuring technique	Temperature range	Main results
	Size (shape)	Concentration						
Bhuiyan et al. [36]	13 nm, 50 nm	0–0.25 vol%	Distilled water	No surfactant	Vibration shaker and ultrasonic homogenizer	Du-Noüy ring method	30–50 °C	ST slightly ↑ with ϕ; ST ↓ with T
Chinnam et al. [6]	20 nm, 45 nm (spherical)	0–6 vol%	PG + W (60 + 40 w/w)	Not indicated type or ionic nature (< 1%)	Ultrasonic bath and probe	Du Nouy maximum pull force method	30–70 °C	ST slightly ↑ with ϕ; ST ↓ with T; ST ↓ with nanoparticle size
Das et al. [29]	38 nm	0–4 vol%	Water	No surfactant	Ultrasonic vibration	Conventional ring method	Room temperature	ST → with ϕ; similar to water
Golubovic et al. [32]	46 nm (spherical)	0–0.01 g/l	Distilled water	No surfactant	Ultrasonic bath	Capillary tube	24 °C	ST → with ϕ; similar to water
Harikrishnan et al. [37]	20 nm (near-spherical)	0–2.5 wt%	Distilled water	No surfactant, CTAB (0, 0.5, 1 CMC)	Ultrasonic probe	Pendant drop method	30 °C	ST ↑ with ϕ
Kim et al. [66]	40–50 nm	0–0.1 vol%	De-ionized water	Unknow (not added during dilution)	Diluted from commercial nanofluid (20 wt%)	Wilhemly-Plate method	20 °C	ST → with ϕ; similar to water
Ranjbar et al. [35]	20 nm, 80 nm	0–10 wt%	Triethylene glycol	No surfactant, Sorbitan oleate (1–10 vol%) for 1 wt% nanofluid based on 20 nm nanopowder	Ultrasonic processor	Pendant drop method	Not mentioned	ST ↓ up to 1%, then ↑; ST ↑ with surfactant; ST ↓ np size
Tanvir and Qiao [34]	25 nm	0–10 wt%	Water	No surfactant	Ultrasonic disruptor	Pendant drop method	Room temperature	ST ↑ with ϕ
Tanvir and Qiao [34]	25 nm	0–10 wt%	Ethanol	No surfactant	Ultrasonic disruptor	Pendant drop method	Room temperature	ST ↑ with ϕ
Tanvir and Qiao [34]	25 nm	0–10 wt%	*n*-decane	Sorbitan Oleate (1 vol%)	Ultrasonic disruptor	Pendant drop method	Room temperature	ST ↓ up to 0.5%, then → and finally ↑ from 4% in ϕ
Zhu et al. [33]	50 nm (near-spherical)	0.1, 1 g/l	Milli-Q Water	No surfactant	Ultrasonic vibrator	Maximum bubble pressure method	294–350 K	ST ↑ with ϕ; ST ↓ with T
Course and Kim [30]	45 nm	0.026–1.02 g/l (water), 0.01–10.02 g/l (ethanol)	Water, ethanol	Unknow concentration	Diluted from commertial nanofluid and vigorously shaken	CA; surface: unoxidized and oxidized	Room temperature	Surface W ↑ with ϕ for fouled surface, shown by CA measurements
Golubovic et al. [32]	46 nm (spherical)	0–0.0065 g/l	Distilled water	No surfactant	Ultrasonic bath	CA; surface: heater wire coated with nanoparticles after boiling	Not mentioned	CA ↑ with ϕ, without size dependence
Jeong et al. [31]	47 nm	0–4 vol%	Water	Not mentioned	Ultrasonic bath	Sensile drop test, surfaces: fresh and quenched steel	Room temperature	Surface W ↑ with ϕ, shown by CA measurements

Table 3
Main informations related to ST and W behavior of TiO_2 nanofluids.

Reference	Nanoparticles		Base fluid	Surfactant	Dispersion method	Measuring technique	Temperature range	Main results
	Size (shape)	Concentration						
Bhuiyan et al. [36]	21 nm	0–0.25 vol%	Distilled water	No surfactant	Vibration shaker and ultrasonic homogenizer	Du-Noüy ring method	303–323 K	ST ↑ with ϕ; ST ↓ with T
Chinnam et al. [6]	15 nm	0–1.5 vol%	PG + W (60 + 40 w/w)	Not indicated type or ionic nature (< 1%)	Ultrasonic bath and ultrasonic probe	Du Nouy maximum pull force method	303–343 K	ST ↓ with ϕ; ST ↓ with T
Ghos Chaudhuri et al. [41]	135–380 nm, varied by chemical treatment	0–20 mg/l	Ultrapure water	No surfactant	One-step method followed by dilution to obtain desired concentrations	Wilhelmy plate technique	301 K	ST ↑ up to 16 mg/l, then ↓; ST (0.8 mg/l) ↑ with np size (plateau 180–340 nm)
Lu et al. [42]	20 nm	1 vol%	PDMS500	No surfactant	Ultrasonic bath	Wilhelmy plate method	298 K	ST → with time
Radiom et al. [40]	15 nm	0–2 vol%	Deionized water	No surfactant, Oleic acid (0.01 and 0.05 vol %)	Mechanical stirring and sonication	Pendant drop method	298 K	ST ↓ with ϕ
Saptoro et al. [44]	7 nm	0–1 wt%	Distilled water	No surfactant	Ultrasonic bath	Drop shape analysis	293–353 K	ST ↓ with T
Ghos Chaudhuri et al. [41]	135–380 nm, varied by chemical treatment	0–20 mg/l	Ultrapure water	No surfactant	One-step method followed by dilution to obtain desired concentrations	Sessile drop technique; Surfaces: glass and PTFE	301	CA on PTFE ↓ with ϕ and nanoparticle diameter; CA on glass more complex
Lu et al. [42]	20 nm	1 vol%	PDMS500	No surfactant	Ultrasonic bath	Drop spreading method	Room temperature	W ↓ with ϕ
Murshed et al. [38]	15 nm (spherical)	0.1 vol%	Deionized water	No surfactant	Ultrasonic dismembrator	Weight-based technique, IT fluid: mineral oil.	298–328 K	ST ↓ with ϕ; ST ↓ with T; IT ↓ with ϕ; IT ↓ with T
Radiom et al. [40]	15 nm	0–2 vol%	Deionized water	No surfactant, Oleic acid (0.01 and 0.05 vol %)	Mechanical stirring and sonication	Sessile drop method; Surface: borosilicate glass	Room temperature	CA ↑ with ϕ

systems can be improved by the use of nanoparticles while this improvement is not achieved with initial better systems. Wetting was also enhanced with water-based nanofluids only if surface is fouled by nanoparticles.

The influence of Al_2O_3 nanoparticle content on the wettability of heated surface under pool boiling was experimentally studied in [31]. In this way, water based nanofluids were produced with Al_2O_3 nanoparticle with 47 nm in mean diameter and 4–124 nm distribution range under volume content of 0–4%. Surface wettability was assessed from contact angle evaluated from sessile drop tests at both ambient pressure and temperature. Nanofluid CA experiments were carried out using fresh steel and quenched steel surfaces as supports and taking care of removing excessive liquid at the surface. It was shown that CA decreases with nanoparticle content.

ST of commercial Al_2O_3 spherical nanoparticles with average diameter of 46 nm dispersed in distilled water was measured by Golubovic et al. [32]. They reported that ST of Al_2O_3 water-based nanofluids at 24 °C, evaluated from capillary tube technique, does not change with nanoparticle content in the range 0–0.01 g/l and is quite similar to that of water. In addition, they investigated the coating of heater surface in nanofluids boiling experiments and reported that CA of nanofluids decreases from 90° to 35.5° with nanoparticle content without effect of nanoparticle diameter, as both trend and value of CA with smaller nanoparticles at same content are identical. So, roughness of boiling surface is linked to nanoparticle deposition and initial concentration in nanoparticles.

Maximum bubble pressure method was used by Zhu et al. [33] to investigate ST of Al_2O_3 water-based nanofluids for two concentrations, 0.1 and 1 g/l, respectively, and temperature range from 294 to 350 K. Nanoparticles were quite spherical in form with unimodal distribution and average size of 50 nm. The authors demonstrated that ST of nanofluids decrease with temperature increase with similar trend than water. ST is increased with nanoparticle content, maximum enhancement of 5% in comparison to water was obtained at 294 K and 1 g/l.

Al_2O_3 with an average diameter of 25 nm were considered by Tanvir and Qiao [34] who produced nanofluids considering water, ethanol and n-decane as base fluids. From pendant drop method, they showed that ST of nanofluids mainly increases with nanoparticle content in the range 0–10% in wt. With n-decane, for which surfactant is used to obtain good dispersion, ST first decreases up to 0.5%, then reaches a plateau up to 4% and finally increases with nanoparticle content. Increase of nanofluid ST in comparison with base fluid was mainly effective from 3 to 4 in wt%.

Two spherical Al_2O_3 nanopowders with average particle sizes of 20 and 80 nm were used by Ranjbar et al. [35] to prepare TEG-based dispersions at nanoparticle concentrations up to 10 wt% and without surfactant addition. ST, evaluated from pendant drop method, was shown to first decrease up to 1 wt%, and then increase up to 10 wt%. Due to the loss of stability after one hour, in a second part of the study authors analyzed the effect that the addition of sorbitan oleate has on the ST of 1 wt% nanofluid based on the nanopowder with the smallest average diameter. Consequently, ST was reduced due to adsorption of surfactant at nanoparticle surface. Some thermodynamic models were favorably compared with their experimental data.

The influence of nanoparticle diameter (20 and 45 nm) and temperature on ST of Al_2O_3 water based nanofluids was investigated by Chinnam et al. [6]. Base fluid was PG/W (60:40 in mass) and ST was experimentally obtained from maximum pull force method and temperature conditions from 30 up to 70 °C. A linear decreasing of ST with temperature was shown for all concentrations, ST also decreases with nanoparticle content and it is lower with smaller size of nanoparticles. Linear fits were proposed to correlate experimental data as it will be shown later in Section 6.

More recently, ST of Al_2O_3 water based nanofluids has been evaluated by Bhuiyan et al. [36] from De-Noüy method in the temperature range 30–50 °C. It was shown also that ST linearly decreases with

Table 4
Main informations related to ST and W behavior of SiO_2 nanofluids.

Reference	Nanoparticles		Base fluid	Surfactant	Dispersion method	Measuring Technique	Temperature range	Main results
	Size (shape)	Concentration						
Bhuiyan et al. [36]	5–15 nm, 10–20 nm	0–0.25 vol%	Distilled water	No surfactant	Vibration shaker and ultrasonic homogenizer	Du-Noüy ring method	30–50 °C	ST ↑ with ϕ; ST ↓ with T
Bhuiyan et al. [43]	5–15 nm	0–0.25 vol%	Methanol	No surfactant	Vibration shaker and ultrasonic homogenizer	Du-Noüy ring method	30–50 °C	ST ↑ with ϕ; ST ↓ with T
Chinnam et al. [6]	20 nm, 30 nm (spherical)	0–6 vol%	PG + W (60 + 40 w/w)	Not indicated type or ionic nature (< 1%)	Diluted from parent sample, ultrasonic bath and probe	Du Nouy maximum pull force method	30–70 °C	ST ↓ with ϕ; ST ↓ with T
Lu et al. [42]	20 nm	1 vol% (also 0.5 vol % for PDMS500)	PDMS100, PDMS500, PDMS1000, PEG200, PEG400	No surfactant	Ultrasonic bath	Wilhelmy plate method	20 °C	ST ↑ with ϕ

temperature whatever the concentration and nanoparticle average diameter. A slight increase of ST with nanoparticle content was also noticed with higher value than base fluid.

Finally, very recently, a comprehensive report about ST of several nanofluids including Al_2O_3 nanoparticle with diameter of 20 nm was presented by Harikrishnan et al. [37]. ST of Al_2O_3 water based nanofluids with contents of CTAB of 0, 0.5 and 1 CMC was measured from pendant drop method at 30 °C and reported to increase with nanoparticle content in the range 0.1–2.5 in wt%, with higher value than water.

2.2. TiO_2 nanofluids

ST of water-based TiO_2 nanofluid with 0.1% in vol. and nanoparticle diameter of 15 nm was measured by Murshed et al. [38]. Using weight-based technique, they reported the decrease of nanofluid ST with the increase in temperature within the range 25–55 °C with similar trend than water. They also showed that ST of water is lowered by the presence of nanoparticles. Both phenomena were attributed to the adsorption of nanoparticles at the interface, with similar action of ST reduction as surfactant, and intensification of Brownian motion with temperature leading to the reduction of cohesive energy. In addition, they also evaluated interfacial tension between water/nanofluids and oil from equation developed by [39]. Nanofluid presented a smaller IT in oil compared with water, and IT is also shown to decrease with temperature.

Water-based TiO_2 nanofluids with same nanoparticle diameter were later studied by Radiom et al. [40] considering a wide range of nanoparticle content, between 0.05% and 2% in volume. They also investigated the influence of oleic acid used as surfactant to stabilize the nanoparticle within water. ST of these nanofluids was obtained from the pendant drop method, while the sessile drop method on borosilicate glass sides was used to evaluate the contact angle of nanofluids. Like in Murshed et al. [38], similar trends were reported and explained by same arguments. In addition, surfactant concentration was shown to be more influent than nanoparticle content with regards of ST decrease. Finally, contact angle was shown to increase with nanoparticle concentration. This behavior was attributed to coupled mechanisms such as solid-liquid interface modification by the adsorption of nanoparticle at solid surface and wetting reduction due to the diminution of particles in wedge film under possible nanoparticle agglomeration at high particle content.

ST of TiO_2 nanoparticles dispersed in water was experimentally measured in [41]. The authors investigated in particular the influence of nanoparticle size between around 135 nm and 380 nm, which was varied by chemical treatment. As previously, ST is reduced with the presence of nanoparticles in comparison to pure water. However, ST first increases with nanoparticle content in the range 0.8–16 mg/l, then ST decreases up to 20 mg/l. At fixed concentration of 0.8 mg/l, ST is shown to mainly increase with nanoparticle size with a plateau for nanoparticle diameter between 180 and 340 nm. Concentration and size effects of these TiO_2 nanofluids on wetting behavior of polytetrafluoroethylene (PTFE) and glass surfaces was also reported in this study. Contact angle decreases on PTFE with particle content and diameter. A more complex behavior was reported for contact angle on glass: it first increases with nanoparticle diameter up to 250 nm then decreases. Contact angle increases at 0.8 mg/l, then decreases up to 8 mg/l and finally increases again up to 20 mg/l.

Dynamic wetting and contact angle of different nanofluids considering TiO_2 as well (20 nm in diameter; 1% in vol.) were measured by Lu et al. [42] at 25 °C using the droplet spreading method. They reported in particular the influence of nanoparticle loading and diameter, base fluid, such as PDMS and PEG, and nature of the substrate. ST of TiO_2 nanofluids does not change over time whatever the base fluid. For a broader context, it was shown that dynamic wetting is lowered by nanoparticle content which enhances the ST of nanofluids. A Newtonian-like dynamic wetting behavior was observed by the authors and bulk dissipation was considered to be responsible of dynamic wetting of nanofluids.

The influence of TiO_2 nanoparticle (21 nm) content on ST of water-based nanofluids was investigated in [43] from Du-Noüy ring method in temperature range 30–50 °C and content 0.05–0.25 vol%. ST was shown to increase with nanoparticle loading and to decrease with temperature. This last trend is linked to the reduction of intermolecular forces due to the enhancement of kinetic energy between molecules. Higher increases with nanoparticle loading were reported for TiO_2 than for Al_2O_3 and SiO_2 nanofluids, which was attributed to change in bulk density of used nanoparticles.

TiO_2 nanoparticles of 15 nm in diameter were considered in [6] where the effect of concentration and temperature was also analyzed. Base fluid was PG/W (60:40 in mass) and ST was experimentally obtained from maximum pull force method. The authors observed a linear decrease of TiO_2 nanofluid ST in the temperature range 30–70 °C, ST being also reduced in comparison to base fluid when nanoparticle content is increased.

More recently, Saptoro et al. [44] explored the effect of microwave irradiation to modify the ST of water nanofluids containing TiO_2 nanoparticles of 7 nm in diameter. Surface tension was determined from drop shape analysis, in the range 20–100 °C and mass fraction between 0.1% and 1%. ST values are first increased with microwave treatment. However, after irradiation, final values are found lower than the initial ones.

Table 5
Main informations related to ST and W behavior of other oxide nanofluids.

Reference	Nanoparticles			Base fluid	Surfactant	Dispersion method	Measuring technique	Temperature range	Main results
	Type	Size (shape)	Concentration						
Chen et al. [49]	Fe_2O_3	10–30 nm (spherical)	0, 0.05, 0.1 wt%	Deionized water	PVP (1 wt%)	Not mentioned	Pendant drop method	Room temperature	ST → with ϕ
Chinnam et al. [6]	ZnO	36 nm, 50 nm (cylindrical)	0–6 vol%	PG + W (60 + 40 w/w)	Not indicated type or ionic nature (< 1%)	Ultrasonic bath and ultrasonic probe	Du Nouy maximum pull force method	30–70 °C	ST ↓ with ϕ ST ↓ with T
Golubovic et al. [32]	BiO_2	38 nm	0–0.01 g/l	Distilled water	No surfactant	Ultrasonic bath	Capillary tube	24 °C	ST → with ϕ
Golubovic et al. [32]	BiO_2	38 nm	0–0.009 g/l	Distilled water	No surfactant	Ultrasonic bath	Sessile drop, Surface: heater wire coated with nanoparticles after boiling	not mentioned	CA of surface layer ↓ with ϕ
Harikrishnan et al. [37]	CuO	30 nm (oblate), 80 nm	0–2.5 wt%	Distilled water	No surfactant, SDS, DTAB	Ultrasonic probe	Pendant drop shape	30 °C	ST (without surfactant) ↑ with ϕ; ST with presence of surfactant ↓ with ϕ
Harikrishnan et al. [37]	MgO	~ 100 nm (disk)	0–2.5 wt%	Distilled water	No surfactant, SDS	Ultrasonic probe	Pendant drop shape	30 °C	ST (without surfactant) ↑ with ϕ; ST with presence of surfactant ↓ with ϕ
Harikrishnan et al. [37]	Bi_2O_3	Thickness: 13–16 nm; Length ~ 300 nm (flake)	0–2.5 wt%	Distilled water	No surfactant, SDS, CTAB	Ultrasonic probe	Pendant drop shape	30 °C	ST (without surfactant) ↑ with ϕ; ST with presence of surfactant ↓ with ϕ
Harikrishnan et al. [37]	Bi_2O_3	Thickness: 13–16 nm; Length ~ 300 nm (flake)	0–5 wt%	Ethylene glycol	No surfactant	Ultrasonic probe	Pendant drop shape	30 °C	ST → with ϕ
Harikrishnan et al. [37]	Bi_2O_3	Thickness: 13–16 nm; Length ~ 300 nm (flake)	0–5 wt%	Glycerol	No surfactant	Ultrasonic probe	Pendant drop shape	30 °C	ST → with ϕ
Harikrishnan et al. [37]	ZnO	80 nm (hexagonal pillar)	0–2.5 wt%	Distilled water	No surfactant, SDS	Ultrasonic probe	Pendant drop shape	30 °C	ST (without surfactant) ↑ with ϕ; ST with presence of surfactant ↓ with ϕ
Harikrishnan et al. [48]	ZnO, CuO, Bi_2O_3	CuO: 30 nm (oblate), 80 nm; ZnO: 80 nm; Thickness: 13–16 nm; Length ~ 300 nm (flake)	0–2.5 wt%	Distilled water	No surfactant, SDS, CTAB	Ultrasonic probe	Sessile drop, Surface: different natures and roughness	30 °C	CA ↓ with ϕ for hydrophilic surfaces; CA ↑ with ϕ for glass and silicon surfaces; With surfactant, CA ↓ with ϕ whatever the surface
Moosavi et al. [47]	ZnO	67 nm	0–3 vol%	Glycerol	No surfactant	Mechanical stirring	Du-Noüy ring method	Room temperature	ST ↑ with ϕ
Pantzali et al. [46]	CuO	30 nm	0–8 vol%	Distilled water	Unknow (not added during dilution)	Diluted from commercial nanofluid (50 wt%) and mechanical stirring	Pendant drop method	25 °C	ST ↓ with T
Saptoro et al. [44]	Fe_2O_3	15 nm	0–0.5 wt%	Distilled water	No surfactant	Ultrasonic bath	Drop size analysis	20–100 °C	ST ↓ with microwave power and duration

2.3. SiO_2 nanofluids

To a smaller extend, very few studies reported ST of SiO_2 nanofluids. The effect of SiO_2 nanoparticle content and size (5–15 nm and 10–20 nm) on this property was investigated by Bhuiyan et al. [36] considering water as base fluid. Experiments were performed using Du-Noüy ring method. The authors evidenced that ST of nanofluids increases with nanoparticle volume fraction in the range 0.05–0.25%, with higher value than base fluid, and decreases linearly with temperature rise between 30 and 50 °C. In comparison to Al_2O_3 and TiO_2 nanoparticle at same content, ST of SiO_2 nanofluids is lower because of the difference in bulk density. They also showed that ST is lowered by nanoparticles with smaller size. Similar effects of temperature and nanoparticle content were presented for smaller size of SiO_2 nanoparticles dispersed in methanol as base fluid [45].

The influence of SiO_2 nanoparticle content and average size (20 nm and 30 nm) on nanofluids ST was also studied by Chinnam et al. [6] from maximum pull force method. Here, nanofluids with required volume fractions were produced by the dilution of parent nanofluids with base fluid, which consists of a mixture of PG and W with the mass ratio 60:40. As for all nanofluids they studied, the authors evidenced the linear decrease of SiO_2 nanofluids ST with temperature for all tested concentration 0–6% in volume. A linear decrease of SiO_2 nanofluids ST with volume content was also reported. ST is also lowered with smaller nanoparticles.

2.4. Other oxide nanofluids

Commercial aqueous nanofluid containing CuO nanoparticles with a mean diameter of 30 nm was investigated by Pantzali et al. [46]. Nanofluids with concentration range between 2% and 8% in volume were prepared from dilution of initial suspension with distilled water. Their ST was measured using pendant drop method at 25 °C and was shown to decrease with nanoparticle loading. The authors also attributed the low value of nanofluid ST in comparison to water to the possible presence of surfactant as stabilizer in the commercial suspension.

ST of ZnO/EG nanofluids was evaluated from the ring method by Moosavi et al. [47]. Mean particle size of ZnO nanoparticles was reported to be around 67 nm. In the range 1–3% in volume fraction, ST of nanofluids was shown to increase with nanoparticle content. A maximum enhancement of 7% in ST compared to EG was reported for the highest concentration.

Recently, a comprehensive report about ST of oxide nanofluids was presented in [37]. In this well detailed study, several types of oxide nanopowders with different morphologies were considered, CuO with oblate shape and average size of 30 nm, MgO disks with variable sizes between 100 and 150 nm, and ZnO with hexagonal structure and average size of 50 nm. The nanoparticles were dispersed in water, known as polar solvent, with and without surfactants, varying also their nature and content. Pendant drop experiments were performed at 30 °C to investigate ST of nanocolloids considering the sole effect of nanoparticle and surfactant content and combined effect of these two parameters. First, they showed that ST of water is increased with nanoparticle content and that ST is also governed by nanoparticle morphology. Enhancement in ST is therefore attributed to the interaction between particle and fluid molecules, which strengthens with high nanoparticle volume ratio. Presence of surfactant decreases ST value of water up to CMC. Most interesting is the combined effect of surfactant and nanoparticle which leads to the decrease of water ST. The higher the content in both nanoparticle and surfactant, the higher is the reduction in ST. This trend was explained and modeled by the authors with the help of Gibbs adsorption theory. It should be finally pointed out that no clear effect of surfactant and CuO nanoparticle content on ST of nanofluids was noticed by the authors using weakly polar base fluid such as EG and glycerol. Similar conclusions about the role of base fluid and presence of surfactant were also obtained by the same authors with Bi_2O_3.

Same group of authors investigated also W of same nanofluids, e.g., ZnO, CuO and Bi_2O_3 in [48] with consideration of nanoparticle loading and both nature and roughness of substrate. They showed that CA of nanofluids mainly decreases with nanoparticle concentration for aluminum and copper substrates. Opposite effect was reported for silicon and glass substrates. With the addition of surfactant, it was shown that CA mainly decreases with nanoparticle concentration whatever the substrate, evidencing the dominant role of surfactant in wettability.

Fe_2O_3 water-based nanofluids were also investigated in [49]. The authors showed that surface tension of nanofluids remains constant with nanoparticle concentration, without dissociating the effect of particles alone, as without PVP nanofluids was not stable. Same nature of nanoparticles were also studied by Saptoro et al. [44], water being used as base fluid. They focused on the effect of microwave irradiation treatment on surface tension of nanofluids, measured from pendant drop method, considering the influence of nanoparticle loading, microwave power and duration. They demonstrated that ST of Fe_2O_3 nanofluids is lowered by microwave treatment increase in power and duration.

3. Carbon-based nanofluids

Main results of surface tension and wettability of carbon-based nanofluids are presented in the following, while details about these studies are summarized in Tables 6 and 7. This section is divided in two parts considering nanotubes and graphene flakes or nanoplatelets, respectively.

3.1. Nanotubes-based nanofluids

ST and contact angle measurements of acid-treated carbon nanotubes dispersed in water without surfactant were reported by Xue et al. [50]. Experiments were performed from bubble pressure method and sessile drop method, by the deposition of droplets on sheet of copper used in heat pipe, for nanotube volume concentration of 1%. Presence of nanotubes increases ST of water up to 13.5% and ST of nanofluid decreases within the temperature range 298.15–343.15 K. It was also shown that nanotubes increase CA values and these are sensitive to drop size.

Effect of chemical treatment and surfactant (SDBS) in the dispersion of SWCNTs in water and surface tension of resulting nanofluids were investigated by Kumar and Milanova [51], and Murshed et al. [52]. A concentration of 0.1% in volume was considered by the authors and bubble pressure method was used. They showed that surfactant content increase within water reduces ST. For nanofluids, ST is quite constant for low content in surfactant which is mainly adsorbed at nanotube surface and serves as stabilizer. However, after surfactant concentration overcomes a critical value, ST decreases because of the excess of surfactant molecules in water. Interestingly, decrease of nanofluid ST with surfactant content was correlated to the increase of heat flux during pool boiling.

Pendant drop method was exploited by Tanvir and Qiao [34] to measure the ST of MWCNTs with average dimensions of 8–15 nm in diameter and 10–50 μm in length dispersed in water and ethanol respectively without the help of surfactant. A concentration range between 0.1% and 10% in mass content was studied and measurements were done at ambient temperature. It was found that ST of water-based nanofluids increase with nanotube mass content. For ethanol-based nanofluids, ST slightly decreases up to 2 wt%, then ST is increased with nanoparticle content.

A well detailed study about the influence of nanofluid stability and stabilization methods used for the production of functionalized MWCNT nanofluids on their wettability and ST was recently reported by Karthikeyan et al. [53]. Water and ethanol were used as base fluids, ST properties were obtained from pendant drop method at ambient temperature. They highlighted that ST of well-stable nanofluids does

Table 6
Main informations related to ST and W behavior of carbon nanotube nanofluids.

Reference	Nanoparticles			Base fluid	Surfactant	Dispersion method	Measuring technique	Temperature range	Main results
	Type	Size (shape	Concentration						
Karthikeyan et al. [53]	Plasma functionalized MWCNT-	Diameter: 35 nm; Length: 3.5 μm,	0–120 ppM	Reverse osmosis water	No surfactant	Sonicated only one during preparation	Pendant drop method	Room temperature	ST → with ϕ
Karthikeyan et al. [53]	Plasma functionalized MWCNT-	Diameter: 35 nm; Length: 3.5 μm,	0–120 ppM	Reverse osmosis water	No surfactant	Sonicated only one during preparation	Sessile drop, Surface: ultra-flat silicon wafer	Room temperature	CA → with ϕ for stable nanofluids
Karthikeyan et al. [53]	Plasma functionalized MWCNT-	Diameter: 35 nm; Length: 3.5 μm,	0–3500 ppM	Ethanol	No surfactant	Sonicated only one during preparation	Pendant drop method	Room temperature	ST → with ϕ up to 500 ppm then ↑
Kumar and Milanova [51], Murshed et al. [52]	SWCNTs	Not mentioned	0, 0.1 vol%	Deionized water	SDBS (0.186–3.735 mM)	Cup-and-horn-type ultrasonicator	Bubble pressure method	Not mentioned	ST ↓ with surfactant content after critical concentration
Tanvir and Qiao [34]	MWCNTs	Diameter: 8–15 nm; Length: 10–50 μm	0–10 wt%	Water	No surfactant	Ultrasonic disruptor	Pendant drop method	Room temperature	ST ↓ with ϕ
Tanvir and Qiao [34]	MWCNTs	Diameter: 8–15 nm; Length: 10–50 μm	0–10 wt%	Ethanol	No surfactant	Ultrasonic disruptor	Pendant drop method	Room temperature	ST ↓ up to 2 wt% then ↑
Xue et al. [50]	Covalent-functionalized CN	Diameter: 15 nm; Length: 10 μm	0, 1 vol%	Distilled water	No surfactant	Ultrasonic applicator	Bubble pressure method	25–70 °C	ST ↑ with ϕ ST ↓ with T
Xue et a. [50]	Covalent-functionalized CN	Diameter: 15 nm; Length: 10 μm	1 vol%	Distilled water	No surfactant	Ultrasonic applicator	Sessile drop method; Surface: copper sheet	25 °C	CA ↑ with ϕ; CA sensitive to size

Table 7
Main informations related to ST and W behavior of graphene nanofluids.

Reference	Nanoparticles			Base fluid	Surfactant	Dispersion method	Measuring technique	Temperature range	Main results
	Type	Size (shape)	Concentration						
Cabaleiro et al. [57]	GO, rGO	5–10 μm, Thickness: 2–10 at. layers	0–0.1 vol%	Water	No surfactant	Ultrasonic bath	Pendant drop technique	Room temperature	ST ↓ with ϕ
Zheng [54]	Not mentioned	14 nm, 30 nm, 80 nm	0–1 wt%	Water	Not mentioned	Not mentioned	Ring method	20–60 °C	ST ↑ with ϕ ST ↓ with T
Ahammed et al. [56]	G	Thickness: 1–5 nm	0–0.15 vol%	Water	SDBS (5 vol% of nanoparticle vol. content)	Ultrasonic vibrator	Bubble pressure method	10–90 °C	ST ↑ with ϕ ST ↓ with T; CA ↑ with ϕ and after boiling
Kamatchi et al. [55]	rGO	Thickness: 2–6 at. layers	0–0.3 g/l	Distilled water	SDBS (5 vol% of nanoparticle vol. content)	Ultrasonic vibrator	Bubble pressure method	35–75 °C	ST ↓ with ϕ ST ↓ with T

not depend on nanotube content for water, and starts only to increase from a critical value of 500 ppm with ethanol as base fluid. Wetting behavior of non-functionalized MWCNTs dispersed in water depends on the use of surfactant. Contact angle of nanofluids on silicon surface is modified with the presence of agglomerates within unstable nanofluids, while contact angle is more affected by the presence of surfactant than nanoparticle content with stable nanofluids (Table 8).

3.2. Graphene-based nanofluids

As for nanotubes, few data for ST of graphene-based nanofluids are available in the literature. First study related to surface tension of graphene-based nanofluid was reported by Zheng [54]. This author investigated the influence of nanoparticle size ranging from 14 to 80 nm (mentioned as a diameter in his work), nanoparticle weight content from 0.06% to 0.1% and temperature between 293 and 333.15 K. It should be noted that information related to graphene oxide type used in the study and experimental procedure for nanoparticle dispersion within water to produce nanofluids were not detailed by the author. ST measurements were performed by using the ring method, experimental device being calibrated with water with a maximum relative deviation of 1.2%. As a result, it was mainly reported that ST of water-based graphene oxide nanofluids increase with nanoparticle content, with a maximum enhancement of 2.98% in comparison to water for 0.1% in wt. content. ST was decreased when the temperature rises and when the nanoparticle size is reduced. Finally, ST reduction rate with temperature was lowered by the presence of nanoparticles.

Later, Kamatchi et al. [55] measured the ST of reduced graphene oxide (rGO) dispersed in water without surfactant considering the effect of nanoparticle concentrations (0.01, 0.1 and 0.3 g/l) and temperatures from 308.15 to 348.15 K. These ST measurements were obtained with a bubble pressure tensiometer with an accuracy of 0.1%. rGO was produced by the reduction of commercial graphite from the modified Hummer method. ST of nanofluids is higher than the one of water and was shown to increase with nanoparticle content. This trend was attributed to the increase in surface energy due to displacement and accumulation of rGO nanoflakes at liquid-gas interface. A decrease in ST of nanofluids with temperature was also observed. In addition to ST, the authors reported also the effect of boiling on wettability of copper surface with same nanofluids from contact angle measurement with sessile drop method. They showed that CA of nanofluids is increased with nanoflake concentration and, unlike water, CA is higher after boiling process.

The dependence of volume concentration (0.05–0.15%) and temperature (10–90 °C) on ST of graphene-water nanofluids was also recently investigated by Ahammed et al. [56]. Commercial graphene with 1–5 nm of thickness was here used and dispersed in water using SDSB as surfactant with content of 5% of each tested nanoparticle volume content. Measurements were performed with a bubble pressure device under an accuracy of 2%. The authors showed that ST of nanofluids both decreases with nanoparticle content and temperature. These trends were explained, respectively, by the enhancement of nanoparticle absorption at liquid-gas interface as graphene is hydrophobic, and by the molecular attraction reduction between fluid molecules and nanoparticles. The reduction rate in temperature was reported to be around 3.3% for each 10 °C increase. It should be mentioned that the sole effect of surfactant on ST of water was not studied by the authors. Therefore, the previous results include combined effects of surfactant and nanoparticles.

Lastly, Cabaleiro et al. [57] investigated the effect of nanoparticle loading and graphene functionalization on surface tension of graphene aqueous nanofluids. GO and two different reduced GO at six nanoparticle volume fractions ranging from 0.0005% to 0.1% were studied. Surface tension measurements were carried out at room temperature from the pendant drop technique. It was observed that surface tension decreases with graphene loading for all nanofluids, with a maximum

Table 8
Main informations related to ST and W behavior of metal nanofluids.

Reference	Nanoparticles			Base fluid	Surfactant	Dispersion method	Measuring technique	Temperature range	Main results
	Type	Size (shape)	Concentration						
Chen et al. [49]	Ag	10–30 nm (spherical)	0.04 wt% (w/o PVP), 0.05 wt% (with PVP)	Deionized water	No surfactant, PVP (1 wt%)	Produced by lass ablation	Pendant drop method	Room temperature	ST ↓ with evaopration
Lee et al. [59]	Ag	50 nm	5–35 wt%	W + DG (50 + 50 w/w)	PVP (7.95 g/g Au used for synthesis)	One step in water + ultrasonic bath	Du Noüy ring method	20 °C	ST ↑ with ϕ
Lu et al. [60]	Au	0.8 nm	0–9.81 vol%	Water	No surfactant	Theoretical research	Theoretical research (32-atom system)	300 K	ST (without surfactant) ↑ with ϕ; ST with presence of surfactant ↓ with ϕ
Sefiane et al. [67]	Al	Not mentioned	0–5 wt%	Ethanol	Not mentioned	Ultrasonic bath	Pendant drop method	Room temperature	ST slightly ↓ with ϕ
Sefiane et al. [67]	Al	Not mentioned	0–5 wt%	Ethanol	Not mentioned	Ultrasonic bath	sessile drop, Surface: pyrex dish	Room temperature	CA ↑ with ϕ up to 1% then ↓
Tanvir and Qiao [34]	Al	18 nm	0–10 wt%	Ethanol	No surfactant	Ultrasonic disruptor	Pendant drop method	Room temperature	ST ↑ with ϕ
Tanvir and Qiao [34]	Al	18 nm	0–10 wt%	*n*-decane	Sorbitan Oleate (1–10 vol% for 0.1 wt% of Al and 1 vol% for the rest)	Ultrasonic disruptor	Pendant drop method	Room temperature	ST ↑ with ϕ; ST ↓ with surfactant content
Tanvir and Qiao [34]	B	80 nm	0–10 wt%	Ethanol, n-decane	No surfactant	Ultrasonic disruptor	Pendant drop method	Room temperature	ST ↑ with ϕ
Vafei et al. [58]	Au	5–90 nm	44 µg/ml	Distilled water	Not mentioned	Ultrasonic homogenize	Prediction from contact angle measurements by solving Laplace-Young Eq.	Not mentioned	ST ↓ with nanoparticle size; ST ↓ with increase in applied voltage

Table 9
Main informations related to ST and W behavior of less used nanofluids.

Reference	Nanoparticles			Base fluid	Surfactant	Dispersion method	Measuring technique	Temperature range	Main results
	Type	Size (shape)	Concentration						
Chen et al. [49]	Laponite	diameter: 25–30 nm, thickness: 1–2 nm, (disk)	0–2 wt%	Deionized water	No surfactant	Not mentioned	Pendant drop method	Room temperature	$ST_{nf} < ST_{bf}$ but ST ↑ with ϕ
Huminic et al. [15]	FeC	14.2 nm	0–1 wt%	Water	Carboxymethyl cellulose sodium salt, CMCNa (3 g/l)	Ultrasonic bath and probe	Du Noüy ring method	10–70 °C	ST ↑ with ϕ ST ↓ with T
Huminic et al. [61]	SiC	25 nm	0–1 wt%	Distilled water	Carboxymethyl cellulose sodium salt, CMCNa (3–10 g/l)	Ultrasonic bath and probe	Du Noüy ring method	20–50 °C	ST ↓ with ϕ ST ↓ with T
Vafei et al. [62]	Bi_2Te_3	2.5 nm, 10.4 nm	$3.1{\cdot}10^{-6}$–$3.2{\cdot}10^{-3}$ g/g	Deionized water	Isooctane/bis-(2-ethylhexyl)-sulfosuccinate, AOT, used for synthesis	Ultrasonic homogenize	Prediction from contact angle measurements by solving Laplace-Young Eq.	Not mentioned	CA ↑ with ϕ up to 1.98 10^{-4} g/g then ↓
Żyła et al. [63]	TiN	20 nm, 50 nm	1–5 wt% (0.22–1.11 vol%)	Ethylene glycol	No surfactant	Ultrasonic bath	Pendant drop technique	293.15 K	ST slightly ↑ with ϕ

reduction of about 3% for the highest volume fraction of 0.1 vol%. However, no clear effect of the chemical reduction on ST of nanofluids was observed.

4. Metallic nanofluids (Au, Ag, Al, B)

Different metallic nanofluids were also considered in some studies, the results are discussed here and compiled in Table 7. Chen et al. [49] analyzed the time dependence of surface tension for aqueous nanofluids prepared using nanoparticle loadings between 0.1 and 2 wt% of laponite disks (diameter 25–30 nm and thickness 1–2 nm) and 0.04 wt% of spherical silver nanoparticles (diameter 10–30 nm) without any surfactant assistance. Authors also studied a nanofluid prepared using 0.05 wt% of Ag nanoparticles using 1 wt% of PVP. A Rame-Hart Model 250 Standard goniometer was used to perform measurements. A droplet of various nanofluids was investigated in time, and during this measurements water evaporates which leads to increase of real fraction of NPs, so actually they measured concentration dependence of surface tension measurements. They concluded that surface tension of the studied nanofluids decreases during evaporation and this phenomenon was opposite to the trend predicted by the Stefan formula, which relates ST and heat of vaporization in the case of pure molecular fluids.

In other paper, Vafaei et al. [58] presented results of experiments on liquid-gas surface tension of water based nanofluids containing gold nanoparticles with various diameters (from 5 to 90 nm). They investigated the effects of applied voltage and the size of gold nanoparticles on the effective liquid–gas surface tension. Vafaei et al. measured radius of triple line, height, and the location of lateral apex of nanofluids droplet during application of voltage between 0 and 30 V. On the base of Young–Laplace equations they calculated surface tension of nanofluids. They presented that, at zero voltage, surface tension decreases with increase of nanoparticle size. A decrease of ST with increasing of voltage was also presented. Hence they observed that after application of voltage, ST of nanofluids decreases with NPs size in range 5–50 nm then increases reaching the maximum value at 90 nm.

Aluminum and boron particles suspended in ethanol and n-decane were investigated by Tanvir and Qiao [34]. They used popular pendant drop method coupled to the Young-Laplace equation to determine the surface tension of these materials. They prepared samples with nanoparticle mass concentrations of 0.1, 0.5, 1, 2, 3, 4, 5, 7 and 10 wt%, without any surfactant in the case of ethanol-based nanofluids and using 1 vol% concentration of Sorbitan Oleate for n-decane nanofluids. Averaged nanoparticle diameters were 80 and 18 nm for B and Al powders, respectively. In both cases, they reported that ST of nanofluids increases with increasing of mass concentration of nanoparticles. They have connected this phenomenon with a strengthening of Van der Waals force between the accumulated particles at the liquid-gas interface. They presented also results of studies on surface tension of n-decane based nanofluids containing 0.1 wt% Al with various volume fractions of surfactant (Sorbitan Oleate). From these results they concluded that surface tension decreases with increasing of volume fraction of surfactant, to the opposite with findings of Chen et al. [49].

Surface tension is one of important parameters in the case of design of printing ink. Lee et al. [59] presented results of experimental studies on surface tension of silver nanoparticles with size of 50 nm suspended in water and diethylene glycol (DG) co-solvent system. They measured surface tension of ink containing 5–35 wt% of silver nanoparticles at constant temperature of 20 °C with tensiometer K10ST (Kruss, Germany). They found that ST increases with nanoparticle content in the whole measured mass concentration range.

It should be finally noted that one numerical research on surface tension of nanofluids was also performed by Lu et al. [60]. They presented results about simulation of surface tension of water based gold nanofluids. They used molecular dynamic simulations and bulk water films with 4500 water molecules at 300 K and three various gold nanoparticles volume concentrations (3.43%, 6.77% and 9.81%) were

simulated. Nanoparticles were modeled as 32-atom systems with dimension of 0.8 × 0.8 × 0.8 nm^3. They concluded that surface tension of nanofluids is strongly connected with nanoparticles wettability. The addition of surfactant-like nanoparticles increases the molecular spacing on the free surface, which reduces the fluid surface tension while non-surfactant nanoparticles reduce the molecular spacing on the free surface which increases the surface tension.

5. Unusual/less studied nanofluids

Some experimental studies on nanofluids containing nanoparticles, which were not mentioned in previous sections, were also performed. Main results and conclusions for these less used nanofluids are reported thereafter, additional details are also given in Table 9.

Huminic et al. [61] used Sigma force tensiometer to determinate ST of water-based nanofluids containing two mass fractions of SiC nanoparticles (0.5 and 1.0 wt%) in temperature range from 293.15 to 323.15 K. Measurements on this equipment are based on Du Noüy ring method, which involves the interaction of a platinum ring with the test surface. They observed for 0.5 wt% of nanoparticles that surface tension is lower than pure base fluid. For highest examined mass concentration, surface tension is higher than base fluid at temperatures above 293.15 K. They connect this phenomenon with results obtained by Murshed et al. [38] for TiO_2 in water nanofluids and suggest that decreasing in surface tension might be caused by the Brownian motion of nanoparticles in the base fluid.

Huminic et al. examined also another aqueous nanofluid containing 14-nm FeC nanoparticles [15]. In this case, they used three concentrations 0.1, 0.5 and 1.0 wt% and temperature ranging from 283.15 to 343.15 K. Once again Sigma force tensiometer was used to perform measurements. They reported that for each examined nanofluid ST decreases with temperature. It was also presented that for the two first concentrations (0.1 and 0.5 wt%) FeC/water nanofluids exhibit lower ST than pure base fluid. Like for previous described SiC/water nanofluids, this behavior was related to Brownian motion and the accumulation of nanoparticles at the gas–liquid interface. They discussed also possibility that this kind of behavior might be caused by surfactants as suggested [34].

Another water-based Bi_2Te_3 nanofluids were examined by Vafaei et al. [62]. They conducted measurements of liquid–gas surface tension of two sizes (2.5 and 10.4 nm) of Bi_2Te_3 nanoparticles. Effective liquid-gas surface tension was calculated from comparison between experimental droplet shape and prediction of Laplace-Young equation. The observed trends in mass concentration dependence of ST were similar for both examined size of nanoparticles. First ST decrease when nanoparticles concentration increase, and after some critical concentration ST starts to increase. This critical concentration was higher for bigger nanoparticles. They explain this behavior by the fact that the nanoparticles accumulate at the liquid–gas interface. When nanoparticles get to the interface they reduce the effective surface energy, nanoparticles become “trapped” at the interface and, in turn the concentration of nanoparticles on the gas-liquid interface rises.

Recently, Żyła et al. [63] also investigated ST of nanofluids containing two different sizes of nanoparticles. Base fluid was ethylene glycol and nanoparticles were TiN with average size of 20 and 50 nm, respectively. Samples were prepared in mass concentrations from 1% to 5% with 1 wt% step, and it corresponding volume fraction ranges from 0.0022%? to 0.0111%. They employed the pendant drop method to determine surface tension between nanofluids and air at constant temperature of 293.15 K from Young-Laplace equation. For both examined sizes of nanoparticles, it was observed that surface tension of nanofluids increases with volume fraction of solid particles. It was also presented that surface tension is higher for nanofluids containing smaller particles.

6. Existing empirical correlations

In some of previous papers, experimental data have been used to develop theoretical or empirical correlations. Experimental results have also been compared with existing models. These models and correlations are detailed in the following including their validity domain.

First, as water is largely used as base fluid for producing nanofluid, expression of its surface tension in function of temperature is here reminded [64].

$$\gamma = 0.076 - 0.00017T \tag{1}$$

where γ is ST in N/m and T the temperature in Kelvin.

Another relationship for ST of water was proposed by Vargaftik et al. [65] within the temperature range 273.01–458 K.

$$\gamma = 235.8\left[\frac{647.15-T}{647.15}\right]1.256\left[1 - 0.625\left(\frac{647.15-T}{647.15}\right)\right] \tag{2}$$

Based on their experimental results, Zhu et al. [33] have suggested the following equation, Eq. (3), for the linear decrease of Al_2O_3 nanofluid ST with temperature in the range 292–352 K:

$$\gamma = A - BT \tag{3}$$

where A and B are constant linked to each nanoparticle loading.

Murshed et al. [38] have compared experimental data of interfacial tension between TiO_2 water nanofluid (0.1% in vol.) and oil for temperature range 298.15–328.15 K to the model developed by Girifalco and Good [39] and defined by the following equation:

$$\gamma ab = \gamma a + \gamma b\text{-}2\Phi\sqrt{\gamma a \gamma b} \tag{4}$$

Here γ_a and γ_b are the surface tensions of both phases a and b respectively, γ_{ab} is the interfacial tension between both phases, and Φ is a constant equals to the ratio of adhesion and cohesion of two phases.

After suggesting some correlations dissociating each studied nanofluid and concentration, Chinnam et al. [6] have proposed a wider correlation based on all experimental data and the additional combination of volume fraction, temperature and average particle size. This correlation was developed for ZnO, Al_2O_3, SiO_2 and TiO_2 nanofluids produced with PG/W (60:40) as base fluid. The equation is valid for temperature range 303–343 K, nanoparticle loading between 0.005 and 0.06 and for nanoparticle diameter, d_p, ranging from 15 to 50 nm.

$$\frac{\gamma nf}{\gamma bf} = a\phi + b\left(\frac{T0}{T}\right) + c\left(\frac{dp}{dbf}\right) + D \tag{5}$$

with T_0 = 299 K, a = − 1.02219, b = − 0.27706, c = 0.00063558 and D = 1.17344. nf and bf subscripts stand for nanofluid and base fluid, respectively, and ϕ is the nanoparticle volume loading. Molecular diameter of base fluid, d_{bf}, was taken to 0.543 nm [6].

Based on their experimental data, Ahammed et al. [56] also proposed an empirical correlation for graphene water nanofluids including influence of both temperature (10–90 °C) and nanoparticle concentrations (0.05–0.15% in vol.).

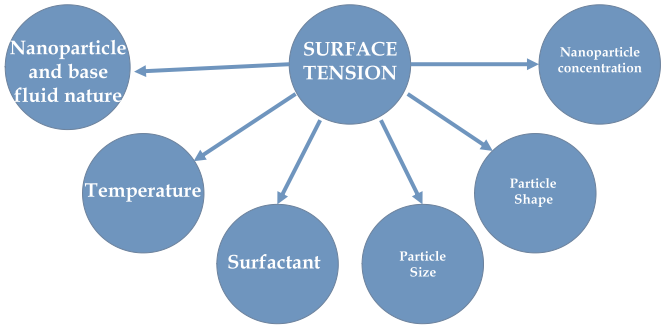

Fig. 2. Factors affecting the surface tension of nanofluids.

$$\frac{\gamma nf}{\gamma bf} = 0.493\left(\frac{T\infty}{Tnf}\right)0.163\left(\frac{1}{\phi}\right)0.0884 \quad (6)$$

In Eq. (6), T_∞ is the ambient temperature and T_{nf} is the temperature of nanofluid.

From a theoretical analysis based on Gibbs adsorption of both surfactant and nanofluids, Harikrishnan et al. [37] developed the following equations for interfacial tension considering their experimental data obtained with CuO nanoparticles dispersed in water with DTAB as surfactant.

$$\gamma xy = \gamma xy0 - \frac{\Gamma xy\infty RT}{nxy}\ln(1+kxyCnxy) \quad (7)$$

where subscript xy denotes any interface between solid-liquid, liquid-gas… γxy is the surface tension at concentration C, γxy0 is the surface tension at zero concentration, R is the universal gas constant and T is the absolute temperature. Γxy∞ represents the limiting surface coverage (basically the maximum possible interfacial concentration of the adsorbate) and kxy is the product of the equilibrium constants for the first and second adsorption steps. Finally, nxy is the fitting parameter linked to the aggregation number [37].

7. Conclusions, challenges and future works

While ST and W are important properties to know and determine in view of the applications of nanofluids in heat exchangers and energy systems, as mentioned in introduction, this review shows that these properties have so far been little studied in comparison to other thermophysical properties. Also, except in few recent works presented before in this paper [6,36,37,48,53], it appears that ST and W of nanofluids are only a part of studies even a complete topic. In addition, there are some issues, which need to be raised.

First, the investigation of ST and W properties must be generalized due to their potential influence in many thermal configurations and technologies, as illustrated in Table 1. In particular, due to the development of high temperature applications with nanofluids, measurements and results have to be produced for temperatures higher than 393.15 K, in particular for liquids and salts used in solar applications.

For lower temperature, the literature overview shows that ST of nanofluids generally decreases with temperature. Avoiding the possible effect of measurement methods and instruments used, this review evidences that ST and W of nanofluids is affected by several parameters, evidenced in Fig. 2, such as nanoparticle nature, shape, size and content. Also, there are some dissenting conclusions regarding the changes in surface tension as a result of the nanoparticle dispersion as ST can increase or decrease with nanoparticle loading following the nature and size/shape of nanoparticles and base fluid. It was also evidenced the great influence of surfactant, because when it is used ST is generally reported to decrease with nanoparticle content. Experimental and theoretical studies have to be performed for a better understanding of influential parameters and development of more universal models and correlations. Moreover, except in few papers, density of nanofluids was not properly given from a theoretical or experimental point of view while this property is needed for ST tension evaluation with all techniques considered. We recommend to systematically include this value in all new coming papers in this topic.

For a practical point of view, some recommendations can also be done. ST can be used as an indicator of nanoparticle stability and dispersion within base fluid following ST value or drop with time. ST and contact angle measurements can also be used in understanding boiling process of nanofluids and deposit of nanoparticles under this process involving surface modifications. These fundamental properties should be further investigated to build a consistent database and help to better understand the two-phase flow behavior and boiling heat transfer characteristics of nanofluids.

Finally, we hope that this overview will be useful for nanofluid community and researchers, and we encourage them to develop studies to fill the gap in this field.

Acknowledgements

This work is a contribution to the COST (European Cooperation in Science and Technology) Action CA15119: Overcoming Barriers to Nanofluids Market Uptake (NanoUptake).

D. Cabaleiro was recipient of a postdoctoral fellowship from Xunta de Galicia (Spain) and acknowledges EU COST for the STMS Grant ref. COST-STSM-CA15119-34906.

G. Żyła acknowledges EU COST for the STMS grant ref. COST-STSM-CA15119-35961.

P. Estellé wishes to acknowledge the European Union through the European Regional Development Fund (ERDF), the Ministry of Higher Education and Research, the French region of Brittany and Rennes Metropole for the financial support related to surface tension device used in some studies presently cited.

D. Cabaleiro and L.Lugo acknowledge the Spanish Ministry of Economy and Competitiveness and EU FEDER Program Project ENE2014-55489-C2-2-R.

References

[1] Incropera FP, DeWitt DP, Bergman TL, Lavine AS. Introduction to heat transfer. sixth ed. New York: John Wiley; 2007.
[2] Parametthanuwat T, Rittidech S, Pattiya A. A correlation to predict heat-transfer rates of a two-phase closed thermosyphon (TPCT) using silver nanofluid at normal operating conditions. Int J Heat Mass Transf 2010;53/21–22:4960–5.
[3] Rohsenow WM. A method of correlating heat transfer data for surface boiling of liquids. Trans ASME 1952;74:969.
[4] Kutateladze SS. On the transition to film boiling under natural convection. Kotloturbostroenie 1948;3:10.
[5] Zuber N, Tribus M, Westwater JW. The hydrodynamic crisis in pool boiling of saturated and subcooled liquids. In: Paper 27 International Dev. in Heat Transfer, ASME, New York; 1961.
[6] Chinnam J, Das DK, Vajjha RS, Satti JR. Measurements of the surface tension of nanofluids and development of a new correlation. Int J Therm Sci 2015;98:68–80.
[7] Lienhard JH, Eichhorn R. Peak boiling heat flux on cylinders in a cross flow. Int J Heat Mass Transf 1976;19:1135–42.
[8] Fang X, Wang R, Chen W, Zhang H, Ma C. A review of flow boiling heat transfer of nanofluids. Appl Therm Eng 2015;91:1003–17.
[9] Ciloglu D, Bolukbasi A. A comprehensive review on pool boiling of nanofluids. Appl Therm Eng 2015;84:45–63.
[10] Vafaei S, Wen DS. Flow boiling heat transfer of alumina nanofluids in single microchannels and the roles of nanoparticles. J Nanopart Res 2011;13(3):1063–73.
[11] Reay D, McGlen R, Kew P. Heat pipes: theory, design and applications. Sixth ed. Oxford: Butterworth-Heinemann; 2014.
[12] Kim BH, Peterson GP. Analysis of the critical Weber number at the onset of liquid entrainment in capillary-driven heat pipes. Int J Heat Mass Transf 1995;38(8):1427–42.
[13] Terdtoon P. et al. Investigation of effect of inclination angle on heat transfer characteristics of closed two-phase thermosyphons, Paper B9P, in: Proceedings of the Seventh International Heat Pipe Conference, Minsk, May; 1990.
[14] Golobič I, Gašperšič B. Corresponding states correlation for maximum heat flux in two-phase closed thermosyphon. Int J Refrig 1997;20(6):402–10.
[15] Huminic AA, Huminic G, Fleaca C, Dumitrache F, Morjan I. Thermal conductivity, viscosity and surface tension of nanofluids based on FeC nanoparticles. Powder Technol 2015;284:78–84.
[16] Liu Z-H, Li Y-Y. A new frontier of nanofluid research – application of nanofluids in heat pipes. Int J Heat Mass Transf 2012;55(23–24):6786–97.
[17] Kumar Gupta N, Kumar Tiwari A, Kumar Ghosh S. Heat transfer mechanisms in heat pipes using nanofluids – a review. Exp Therm Fluid Sci 2018;90:84–100.
[18] Karayiannis TG, Mahmoud MM. Flow boiling in microchannels: fundamentals and applications. Appl Therm Eng 2017;115:1372–97.
[19] Cheng P, Wu HY. Mesoscale and microscale phase-change heat transfer. Adv Heat Trans 2006;39:469–573.
[20] Hao Gu H, Duits MHG, Mugele F. Droplets formation and merging in two-phase flow microfluidics. Int J Mol Sci 2011;12(4):2572–97.
[21] Kandlikar SG. Chapter 5 - flow boiling in minichannels and microchannels. In: Heat transfer and fluid flow in minichannels and microchannels (Second Edition), Butterworth-Heinemann, Oxford; 2014, p. 221–93.
[22] Karniadakis G, Beskok A, Aluru N. Springer, New York, NY; 2006.
[23] Kandlikar SG SG. Heat transfer mechanisms during flow boiling in microchannels. Heat Transf 2004;126:8–16.
[24] Murshed SMS, Nieto de Castro CA. Spreading characteristics of nanofluid droplets impacting onto a solid surface. J Nanosci Nanotechnol 2011;11:3427–33.
[25] Angayarkanni SA, Philip J. Review on thermal properties of nanofluids: recent

developments. Adv Coll Interface Sci 2015;225:146–76.
[26] Murshed SMS, Estellé P. A state of the art review on viscosity of nanofluids. Renew Sustain Energy Rev 2017;76:1134–52.
[27] Drelich J, Fang C, White CL. Measurement of interfacial tension in fluid-fluid systems, Enc Surf Coll Sci. second ed. Boca Raton: CRC Press; 2006.
[28] Berry JD, Neeson MJ, Dagastine RR, Chan DYC, Tabor RF. Measurement of surface and interfacial tension using pendant drop tensiometry. J Coll Int Sci 2015;454:226–37.
[29] Das SK, Putra N, Roetzel W. Pool boiling characteristics of nano-fluids. Int J Heat Mass Transf 2003;46:851–62.
[30] Coursey JS, Kim J. Nanofluid boiling: the effect of surface wettability. Int J Heat Fluid Flow 2008;29:1577–85.
[31] Jeong YH, Chang WJ, Chang SH. Wettability of heated surfaces under pool boiling using surfactant solutions and nano-fluids. Int J Heat Mass Transf 2008;51:3025–31.
[32] Golubovic MN, Madhawa Hettiarachchi HD, Worek WM, Minkowycz WJ. Nanofluids and critical heat flux, experimental and analytical study. Appl Therm Eng 2009;29:1281–8.
[33] Zhu DS, Wu SY, Wang N. Surface tension and viscosity of aluminum oxide nanofluids. AIP Conf Proc 2010;1207:460.
[34] Tanvir S, Qiao L. Surface tension of nanofluid-type fuels containing suspended nanomaterials. Nanoscale Res Lett 2012;7:26.
[35] Ranjbar H, Khosravi-Nikou MR, Safiri A, Bovard S, Khazaei A. Experimental and theoretical investigation on Nano-fluid surface tension. J Nat Gas Sci Eng 2015;27:1806–13.
[36] Bhuiyan MHU, Saidur R, Mostafizur RM, Mahbubul IM, Amalina MA. Experimental investigation on surface tension of metal oxide–water nanofluids. Int Commun Heat Mass Transf 2015;65:82–8.
[37] Harikrishnan AR, Dhar P, Agnihotri PK, Gedupudi S, Das SK. Effects of interplay of nanoparticles, surfactants and base fluid on the interfacial tension of nanocolloids. Eur Phys J E 2017;40:53.
[38] Murshed SMS, Tan S-H, Nguyen N-T. Temperature dependence of interfacial properties and viscosity of nanofluids for droplet-based microfluidics. J Phys D: Appl Phys 2008;41:085502.
[39] Girifalco LA, Good RJ. A theory for the estimation of surface and interfacial energies. I. Derivation and Application to Interfacial Tension. J Phys Chem 1957;61:904–9.
[40] Radiom M, Yang C, Chan WK. Characterization of surface tension and contact angle of nanofluids. In: Quan C, Qian K, Asundi A, Chau FS (eds). Proceedings of the Fourth International Conference on Experimental Mechanics. Proc. of SPIE, vol. 7522, 75221D.
[41] Ghosh Chaudhuri R, Paria S. The wettability of PTFE and glass surfaces by nanofluids. J Coll Interface Sci 2014;434:141–51.
[42] Lu G, Duan Y-Y. Wang X6D. Surface tension, viscosity, and rheology of water-based nanofluids: a microscopic interpretation on the molecular level. J Nanopart Res 2014;16:2564.
[43] Bhuiyan MHU, Saidura R, Amalina MA, Mostafizur RM, Islam A. Effect of nanoparticles concentration and their sizes on surface tension of nanofluids. Proc Eng 2015;105:431–7.
[44] Saptoro A, Kanazawa Y, Asada M, Asakuma Y, Phan C. Microwave Irradiation based non-chemical method to manipulate surface tension of nanofluids. Exp Therm Fluid Sci 2016;72:228–34.
[45] Bhuiyan MHU, Saidur R, Amalina MA, Mostafizur RM. Effect of surface tension on SiO2 methanol nanofluids. IOP Conf Ser: Mater Sci Eng 2015;88:012056.
[46] Pantzali MN, Kanaris AG, Antoniadis KD, Mouza AA, Paras SV. Effect of nanofluids on the performance of a miniature plate heat exchanger with modulated surface. Int J Heat Fluid Flow 2009;30:691–9.
[47] Moosavi M, Goharshadi EK, Youssefi A. Fabrication, characterization, and measurement of some physicochemical properties of ZnO nanofluids. Int J Heat Fluid Flow 2010;31:599–605.
[48] Harikrisnan AR, Dhar P, Agnihotri PK, Gedupudi S, Das SK. Wettability of complex fluids and surfactant capped nanoparticle-induced quasi-universal behavior. J Phys Chem B 2017;121:6081–95.
[49] Chen Ruey-Hung, Tran X Phuoc, Martello Donald. Surface tension of evaporating nanofluid droplets. Int J Heat Mass Transf 2011;54(11):2459–66.
[50] Xue HS, Fan JR, Hu YC, Hong RH, Cen KF. The interface effect of carbon nanotube suspension on the thermal performance of a two-phase closed thermosiphon. J Appl Phys 2006;100:104909.
[51] Kumar R, Milanova D. Effect of surface tension on nanotube nanofluids. Appl Phys Lett 2009;94:073107.
[52] Murshed SMS, Milanova D, Kumar R An experimental study of surface tension-dependent pool boiling characteristics of carbon nanotubes-nanofluids. In: Proceedings of the seventh international ASME conference on nanochannels, microchannels and minichannels. Pohang, South Korea, June 22–24; 2009, ICNMM2009-82204.
[53] Karthikeyan A, Coulombe S, Kietzig AM. Wetting behavior of multi-walled carbon nanotube nanofluids. Nanotechnology 2017;28:105706.
[54] Zheng Z. Experimental investigation on surface tension of water-based graphene oxide nanofluids. Adv Mater Res 2015;1082:297–301.
[55] Kamatchi R, Venkatachalapathy S, Srinivas BA. Synthesis, stability, transport properties, and surface wettability of reduced graphene oxide/water nanofluids. Int J Therm Sci 2015;97:17–25.
[56] Ahammed N, Asirvatham LG, Wongwises S. Effect of volume concentration and temperature on viscosity and surface tension of graphene–water nanofluid for heat transfer applications. J Therm Anal Calorim 2016;123:1399–409.
[57] Cabaleiro D, Estellé P, Navas H, Desforges A, Vigolo B. Dynamic viscosity and surface tension of stable graphene oxide and reduced graphene oxide aqueous nanofluids. J. Nanofluids 2018;7:1081–8.
[58] Vafaei S, Chinnathambi K, Borca-Tasciuc T. Liquid–gas surface tension voltage dependence during electrowetting on dielectric testing of water and 5–90 nm gold nanofluids. J Coll Interface Sci 2017;490:797–801.
[59] Lee H-H, Chou K-S, Huang K-C. Inkjet printing of nanosized silver colloids. Nanotechology 2005;16/10:2436.
[60] Lu G, Duan Y-Y, Wang X-D. Surface tension, viscosity, and rheology of water-based nanofluids: a microscopic interpretation on the molecular level. J Nano Res 2014;16/9:2564.
[61] Huminic G, Huminic A, Fleaca C, Dumitrache F, Morjan I. Thermo-physical properties of water based SiC nanofluids for heat transfer applications. Int Commun Heat Mass Transf 2017;84:94–101.
[62] Vafaei S, Purkayastha A, Jain A, Ramanath G, Borca-Tasciuc T. The effect of nanoparticles on the liquid–gas surface tension of Bi_2Te_3 nanofluids. Nanotechnology 2009;20/18:185702.
[63] Żyła G, Fal J, Estellé P. Thermophysical and dielectric profiles of ethylene glycol based titanium nitride (TiN–EG) nanofluids with various size of particles. Int J Heat Mass Transf 2017;113:1189–99.
[64] Nguyen NT, Wereley ST. Fundamentals and Applications in Microfluidics. 2nd ed. 2006.
[65] Vargaftik NB. International tables of the surface tension of water. J Phys Chem Ref Data 1983;12/3:4.
[66] Kim SJ, Bang IC, Buongiorno J, Hub LW. Surface wettability change during pool boiling of nanofluids and its effect on critical heat flux. Int J Heat Mass Transf 2007;50:4105–16.
[67] Sefiane K, Skilling J, MacGillivray J. Contact line motion and dynamic wetting of nanofluid solutions. Adv Coll Interface Sci 2008;138:101–20.